An MMAC C-Band FET Feedback Power Amplifier

AMIN K. EZZEDDINE, MEMBER, IEEE, HING-LOI A. HUNG, SENIOR MEMBER, IEEE, AND HO C. HUANG, SENIOR MEMBER, IEEE

Abstract—**A new feedback power amplifier using miniaturized microwave active circuit (MMAC) technology has been developed for satellite *C*-band applications. This design demonstrates for the first time that a strong negative feedback can be implemented in the microwave frequencies to improve amplifier linearity and output power over a 750 MHz bandwidth. The amplifier provides a third-order intermodulation distortion improvement of 7 to 9 dB across the band at backoff, compared to results obtained using the conventional approach without feedback. The theory, proof-of-concept experiment, design, and MMAC implementation of the feedback amplifier are presented.**

I. Introduction

POWER AMPLIFIERS with high linearity and efficiency are required for satellite transponder applications. During heavy traffic periods, a few decibels of improvement in the linearity of the existing down-link amplifier can greatly enhance overall system capabilities. Rapid advances in microwave solid-state circuitry have provided several means for improving these parameters [1], [2]. Negative feedback has been used in microwave integrated circuits (MIC's) and monolithic microwave integrated circuits (MMIC's) to improve the bandwidth and the input and output voltage standing-wave ratio (*VSWR*) of small-signal microwave amplifiers [3], [4]. It is also known from radio frequency applications that negative feedback can significantly improve the linearity of power amplifiers. However, no attempt to implement strong negative feedback into an MIC field-effect transistor (FET) power amplifier to improve its linearity and efficiency over a broad bandwidth has been reported. Application of this concept at microwave frequencies over a relatively wide bandwidth is difficult because the small wavelength at these frequencies, and a transfer function with a rapid phase variation associated with conventional power amplifiers, can produce in-band instability.

This paper discusses a miniaturized negative-feedback FET power amplifier which can be completely integrated on a single substrate and fabricated using a miniaturized microwave active circuit (MMAC) batch processing technique. (MMAC is a thin-film process by which substrates with passive elements such as resistors, capacitors, transmission lines, and via holes are manufactured. A detailed explanation of the process is given in Section V.) COMSAT believes that this is the first time the feedback concept has been implemented using short-gate-length power devices with special circuit topology and the MMAC to produce a power amplifier with improved linearity at bandwidths exceeding 500 MHz.

The theory of feedback power amplifiers is discussed, and a proof-of-concept experiment is presented. The amplifier feedback design and model predictions are then outlined, and the MMAC technology and fabrication technique are briefly described. Measured data are presented, and a comparison is made between the amplifier open-loop and closed-loop[1] data.

II. Theory

In order to achieve a reasonable power gain at microwave frequencies, FET's generally require matching circuit elements at both the input and the output of the device. Microwave power FET's have relatively low gain and significant gain rolloff with frequency compared to their low-frequency counterparts such as the bipolar power transistor and the metal–oxide–semiconductor FET (MOSFET), each at its corresponding frequency of operation. Consequently, a power amplifier operating over a large bandwidth has a transfer function with rapidly varying phase characteristics, making it a challenge to achieve stable negative feedback operation over such bandwidths.

FET fabrication technology has advanced to a level where FET's with gate lengths 0.5 μm or less can have reasonable gain at millimeter-wave frequencies. Such high-frequency power FET's can be used at *X*-band and below in a negative-feedback configuration with reasonable bandwidth. Furthermore, with the development of MMIC and MMAC circuits, miniaturization of power amplifiers can significantly reduce the phase transfer characteristics of the feedback path so as to make a negative-feedback power amplifier a reality.

The design of the negative feedback amplifier must follow certain guidelines. First, phase variation of the

Manuscript received May 12, 1989; revised October 25, 1989. This paper is based on work performed at COMSAT Laboratories under the joint sponsorship of the Communications Satellite Corporation and the International Telecommunications Satellite Organization (INTELSAT). Views expressed are not necessarily those of INTELSAT.

The authors are with COMSAT Laboratories, Clarksburg, MD 20871-9475.

IEEE Log Number 8933770.

[1]In this paper, the terms *closed-loop* and *open-loop* refer to amplifier configurations with and without feedback, respectively.

0018-9480/90/0400-0350$01.00 ©1990 IEEE

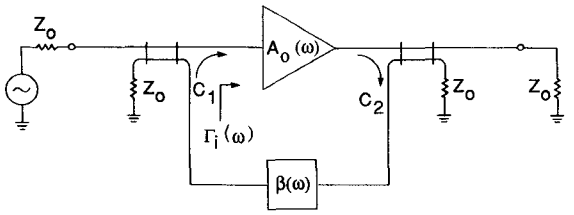

Fig. 1. Feedback amplifier configuration.

open-loop (without feedback) gain should be minimized by properly matching the amplifier stages and by choosing FET's with short gate lengths. This minimum phase variation is essential in order to minimize out-of-band positive feedback which might cause detrimental oscillations. Second, unconditional stability of the amplifier should be obtained at all frequencies. This condition can be achieved by partially matching the input and output of the open-loop amplifier which has a voltage transmission (A_o) to ensure that with the feedback network (β) the closed-loop reflection coefficient (Γ) remains smaller than 1, as

$$\Gamma(\text{closed-loop}) = \frac{\Gamma(\text{open-loop})}{1 - A_o\beta} < 1.$$

Third, the phase of the feedback network should be adjusted to obtain a 180° phase shift at midband. This can be achieved by using a short section of transmission line.

Fig. 1 shows the basic negative-feedback amplifier used for the present study. The voltage transmission of the feedback amplifier, $A_f(\omega)$, can be given as

$$A_f(\omega) = \frac{A_o(\omega)}{1 - A_o(\omega)\beta(\omega)C_1C_2} \tag{1}$$

where

$A_o(\omega)$ voltage transmission of the open-loop amplifier,
C_1 coupling of input coupler ($C_1 < 1$),
C_2 coupling of output coupler ($C_2 \ll 1$),
$\beta(\omega)$ transfer function of the feedback network.

The amplifier input and output reflection coefficients, $\Gamma_{if}(\omega)$ and $\Gamma_{of}(\omega)$, are

$$\Gamma_{if}(\omega) = \frac{\Gamma_i(\omega)}{1 - A_o(\omega)\beta(\omega)C_1C_2} \tag{2a}$$

$$\Gamma_{of}(\omega) = \frac{\Gamma_o(\omega)}{1 - A_o(\omega)\beta(\omega)C_1C_2}. \tag{2b}$$

The ratio of the intermodulation distortion to the signal amplitude, $(D/S)_f$, is

$$\left(\frac{D}{S}\right)_f = \left(\frac{D}{S}\right)\left|\frac{1}{1 - A_o(\omega)\beta(\omega)C_1C_2}\right|. \tag{3}$$

Equations (1), (2), and (3) show that, for negative-feedback operation $|1 - A_o(\omega)\beta(\omega)C_1C_2| > 1$, return losses and distortion are improved over those of the open-loop configuration. By differentiating (1) with respect to ω it can also be shown that the gain flatness improves for negative feedback.

A more accurate analysis of feedback effects should include the open-loop characteristics under large-signal conditions. The output signal, $v_o(t)$, is a nonlinear function of the input signal, $v_i(t)$. (In this paper, slowly varying voltage quantities are represented by capital letters, and rapidly varying voltages are represented by lowercase letters.) For a sinusoidal input, the output voltage spectrum contains the input frequency spectrum, as well as dc and harmonics, as

$$v_o(t) = V_{o,\text{dc}}(t) + \sum_{n=1}^{\infty} |V_{o,n}(t)| \cos(n\omega_c t + \phi_n). \tag{4}$$

The signals, $V_{o,\text{dc}}(t)$ and $V_{o,n}(t)$, are complex functions of the amplitude of the slowly varying real input signal $V_{i,1}(t)$, where $v_i(t) = V_{i,1}(t)\cos\omega_c t$, and ϕ_n is the phase of $V_{o,n}(t)$. For a small signal the amplifier is linear, and consequently

$$v_o(t) = |A_o(\omega_c)|V_{i,1}(t)\cos(\omega_c t + \phi_1) \tag{5}$$

where A_o is the small-signal gain of the amplifier. As $V_{i,1}(t)$ continues to increase, the output becomes a nonlinear function of the input.

The intermodulation distortion (IMD) and AM-to-PM conversion are determined by knowing the characteristics of the function $V_{o,1}(t)$ as a function of $V_{i,1}(t)$, as

$$V_{o,1}(t) = G[V_{i,1}(t), \omega_c] \cdot V_{i,1}(t). \tag{6}$$

The complex variable G is a symmetric nonlinear function of $V_{i,1}(t)$ (for a slowly varying function) and equals $A_o(\omega_c)$ for a small signal. (Symmetry is assumed since the gain is not a function of input phase.) In particular, if G is expanded as a polynomial in $V_{i,1}(t)$ (which is an accurate representation for moderate nonlinearities):

$$G[V_{i,1}(t), \omega_c] = \sum_{N=0}^{\infty} A_N V_{i,1}^{2N}(t). \tag{7}$$

The output, $V_{o,1}(t)$, can be calculated in the case of a sinusoidally modulated input waveform with modulation frequency $f_m = \omega_m/2\pi$:

$$V_{i,1}(t) = V_1 \cos\omega_m t.$$

Hence, as shown in the Appendix,

$$V_{o,1}(t) = \sum_{q=0}^{\infty} B_{2q+1}(V_1)\cos[(2q+1)\omega_m t] \tag{8}$$

where

$$B_{2q+1}(V_1) = \sum_{N=q}^{\infty} \frac{A_N V_1^{2N+1}}{2^{2N}} \binom{2N+1}{N-q}.$$

Note that the output contains the modulation frequency, ω_m, and its odd harmonics, $3\omega_m$, $5\omega_m$, etc. Of particular interest is the carrier-to-third-order intermodulation ratio for two tone carriers:

$$\frac{C}{I_3} = \frac{|B_1(V_1)|}{|B_3(V_3)|}.$$

By performing large-signal power and phase measurements of the output versus input power, the function $G[V_{i,1}(t), \omega_c]$

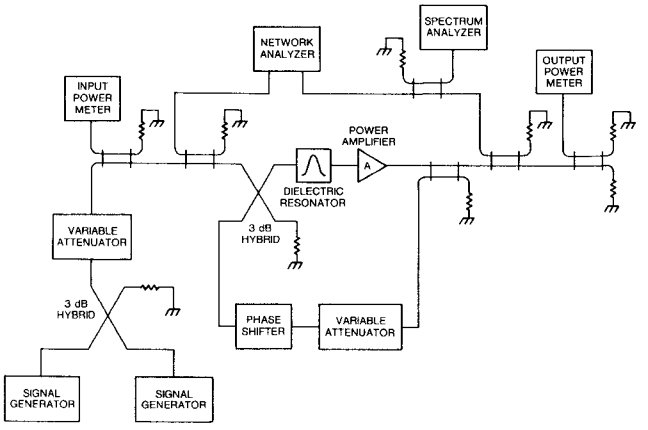

Fig. 2. Proof-of-concept experiment.

is determined. Note that a dependence of the phase of G on $V_{i,1}(t)$ indicates the existence of AM-to-PM conversion, and vice versa.

With feedback, the amplifier output is a function of both input and output, as

$$V_{o,1}(t) = G\{[V_{i,1}(t) - C_1C_2\beta(\omega_c)V_{o,1}(t)], \omega_c\} \cdot [V_{i,1}(t) - C_1C_2\beta(\omega_c)V_{o,1}(t)]. \quad (9)$$

For a sinusoidal input, $V_1 \cos \omega_m t$, the output waveform can readily be calculated using numerical methods and then Fourier-analyzed to find its modulation harmonic frequency content (provided that the carrier harmonic frequencies at the output do not appear at the input).

A computer program was developed to predict the nonlinearities of the feedback power amplifier based on the equations derived in this section. In Section III, the theoretical results are compared with the experimental measured data.

III. Proof-of-Concept Experiment

An experiment was performed using a 5 W FET amplifier module at 4 GHz to study the effect of negative feedback. The experimental setup (Fig. 2) was similar to that used in an experiment by Hsieh and Strid [5] for a power bipolar transistor at S-band.

The network analyzer was essential in the experiment to adjust the 180° phase necessary for negative-feedback operation. A dielectric cavity resonator with a 3 MHz bandwidth and a center frequency at 4 GHz was needed to obtain the proper phase margin for stable amplifier operation. This experimental setup could not provide more than 1 to 2% bandwidth, due to the large phase variation in the amplifier loop. The experiment was performed with both open- and closed-loop operation to compare the output power of the amplifier at 1 dB gain compression and third-order IMD with and without feedback, as described in the theoretical discussion.

Fig. 3 illustrates the output power versus input power of the C-band amplifier module without feedback at 4 GHz, and the output phase deviation from linear phase, $\Delta\phi$. These P_{out} versus P_{in} measured results were used to numerically calculate $V_{o,1}$ (eq. (9)) for two-tone IMD, and a Fourier analysis of the output showed reasonable correlation with measured results for third-order IMD, as shown in Fig. 4.

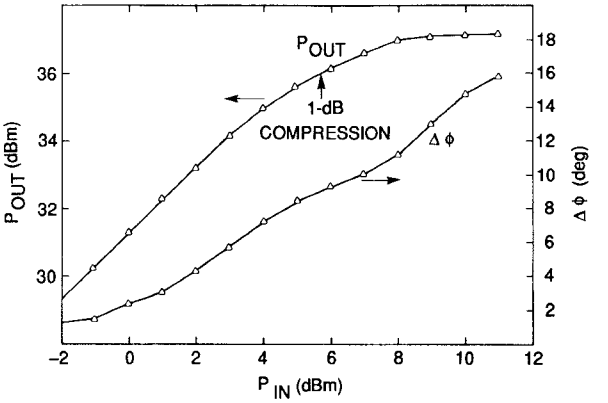

Fig. 3. Measured P_{out} and $\Delta\phi$ versus P_{in} without feedback.

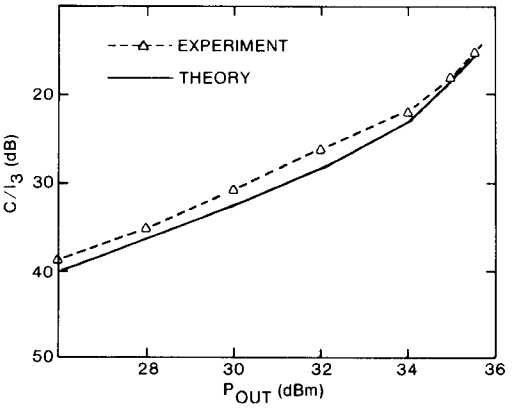

Fig. 4. Predicted and measured C/I_3 versus P_{out} without feedback.

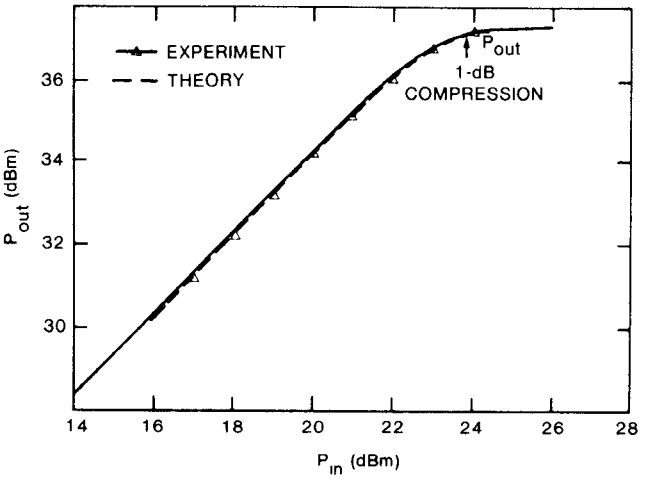

Fig. 5. Predicted and measured P_{out} versus P_{in} with feedback.

With negative feedback, the theory predicts higher output power at 1 dB compression and lower distortion, as illustrated in Figs. 5 and 6, respectively, compared to the open-loop performance shown in Figs. 3 and 4. The calculated output power in Fig. 5 shows good agreement with measurements, and the higher output power 1 dB compres-

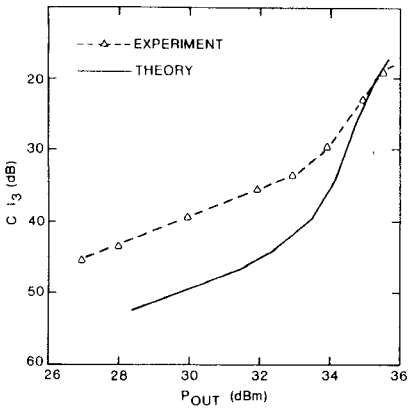

Fig. 6. Predicted and measured third-order IMD versus P_{out} with feedback.

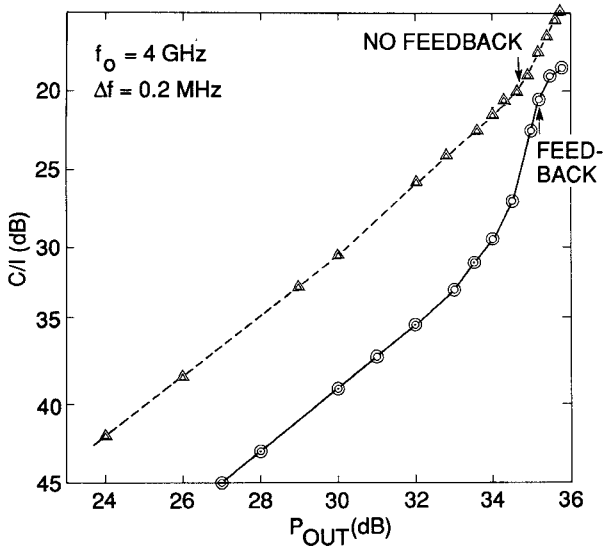

Fig. 7. Third-order IMD for configurations with and without feedback.

sion clearly shows the advantage of negative feedback in obtaining higher power and better linearity.

The open-loop gain of the amplifier was 31.3 dB. The amount of negative feedback was adjusted using the variable attenuator and the phase shifter. The gain of the feedback configuration (closed loop) was 14.3 dB. The output power at the 1 dB gain compression point was 1.25 dB higher for the feedback case, which increased output power by 33%.

The IMD was measured for different levels of input power using two equal carriers with a separation of 0.2 MHz. Fig. 7 shows the third-order IMD versus output power of the amplifier for both cases. The feedback configuration exhibited a marked improvement in carrier-to-intermodulation ratio (C/I) over the open-loop configuration. The measured IMD in Figs. 4 and 6 shows an 8 dB improvement at small signals over the open-loop configuration. At small signals, some deviation occurred in the results from the measurements compared to those from the theoretical calculation. This was caused by part of the second harmonic signal that was returned to the input of the amplifier through the feedback loop. However, at near

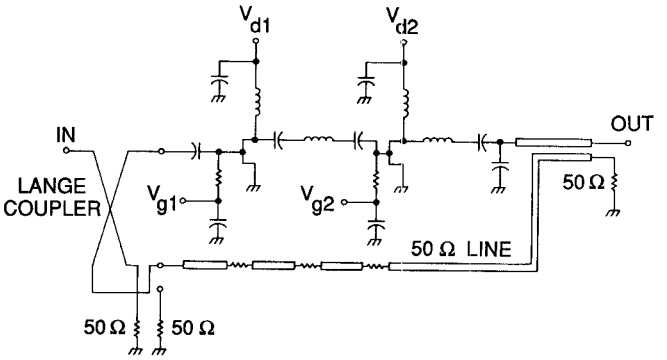

Fig. 8. Schematic of a two-stage feedback power amplifier at *C*-band.

saturation the theory accurately predicted the IMD of the amplifier in both open- and closed-loop configurations.

The present experiment clearly shows a large increase in the output power and an improvement in IMD for the feedback case. Similar conclusions were reported by Takahashi *et al.* [6] for a configuration with a dielectric resonator filter.

IV. Miniaturized Amplifier Design

The amplifier was designed with a circuit topology identical to the configuration shown in Fig. 1. Although the negative feedback could be implemented using a passive low-loss circuit instead of the input and output couplers, the configuration was selected to improve the isolation between input and output, resulting in an unconditionally stable amplifier over the in-band and out-of-band frequencies.

Fig. 8 is a schematic of the two-stage amplifier design with a 3.4–4.2 GHz bandwidth. First, it was experimentally determined that the output-matching network of the power stage presented the optimum load for the COMSAT-developed CST2027 0.5 W FET, a device with a gate length of 0.5 μm. The interstage and input-matching circuits for the two-stage amplifier were then designed using a lower power FET as a driver for the COMSAT FET. Loop gain was adjusted using the length of the coupled lines at the output of the amplifier, and the 180° phase shift in the feedback path was obtained by adding a length of transmission line in the feedback circuit.

The predicted open-loop gain was 19.0 dB at 3.7 GHz, and dropped to 13 dB at the upper band edge, as shown in Fig. 9. The phase margin of the loop was kept greater than 70° by optimizing the amplifier design to satisfy the Nyquist criterion (a necessary condition for stability, but insufficient for unconditionally stable operation). The resistor at the input of the first FET (Fig. 8) was needed to improve the return loss at the input, in order to ensure that the magnitude of closed-loop input return loss, $|\Gamma_{if}(\omega)|$, was smaller than 1. Note that at frequencies when the loop phase is 360°, the denominator in (2a) can be smaller than 1. By achieving a reasonable open-loop input match such that $|\Gamma_i(\omega)|<1$, the occurrence of $|\Gamma_{if}(\omega)|>1$ can be prevented, thus achieving a stable design.

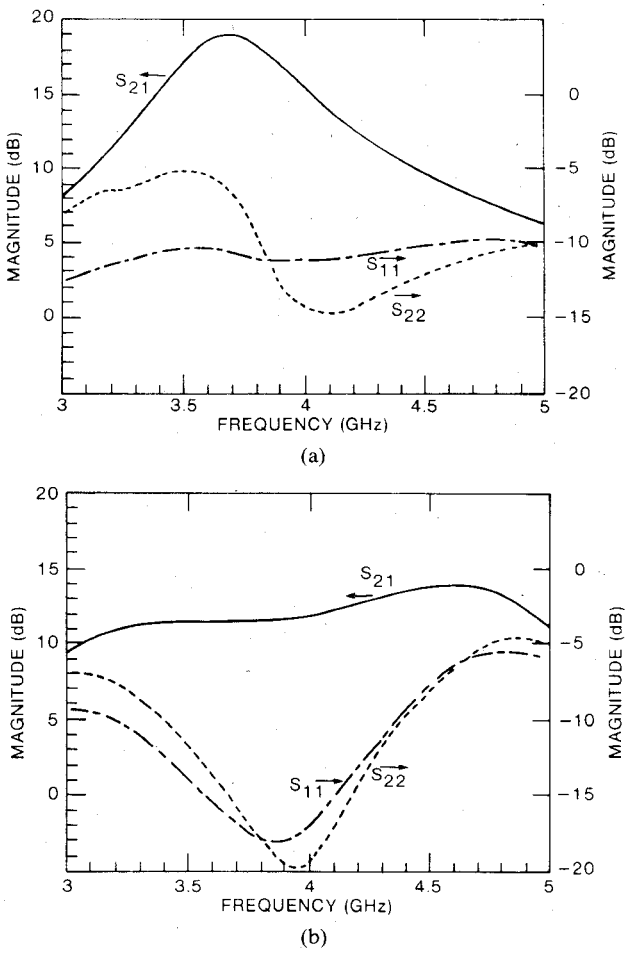

Fig. 9. Predicted gain and return loss versus frequency. (a) Without feedback. (b) With feedback.

As shown in Fig. 9, the largest computer-predicted difference between open- and closed-loop gain occurred at a frequency near midband; therefore, the maximum reduction in third-order IMD is expected. The predicted input and output return losses of the amplifier for the open- and closed-loop conditions are also shown in Fig. 9. These values indicate that negative feedback can significantly improve in-band input and output return losses, as well as amplifier linearity. Outside the band of interest, above 4.2 GHz, the negative feedback becomes ineffective. Consequently, both the return losses and gain flatness are degraded.

V. Fabrication and Circuit Layout

The circuit was fabricated using COMSAT MMAC technology on 10 mil alumina substrate. The MMAC technology is a batch fabrication process, allowing all passive components such as resistors and capacitors, as well as dielectric crossovers and via holes, to be fabricated on a single substrate. The FET device is mounted either on the substrate or through a via hole on a carrier, depending on the thermal dissipation requirement. The substrate used was the type having the minimum inclusion polishing process (MIPP) finish. The use of a highly polished substrate was essential in order to avoid the occurrence of pinholes in the dielectric film.

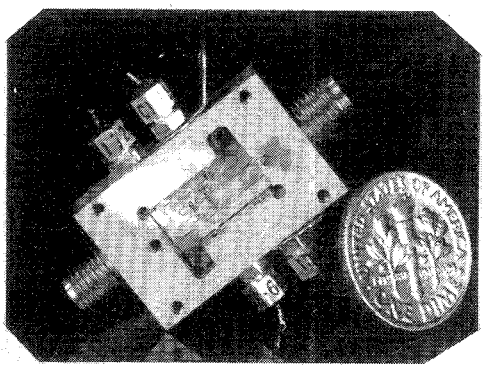

Fig. 10. Two-stage feedback amplifier.

Thin tantalum nitride resistive films were reactively sputtered on the substrate, in a pattern defined by ion-beam milling through the photoresist patterns. The capacitors were fabricated using a titanium–tungsten/gold (Ti–W/Au) layer for the bottom plates. Next, thin-film plasma-enhanced chemical vapor deposition (PECVD) silicon nitride (Si_3N_4) dielectric was deposited over the entire substrate. This layer was then patterned by reactive ion etching (RIE) to leave silicon nitride islands covering the previously defined bottom plate. A thin layer of gold was then evaporated, defining the capacitor top plates and dielectric bridge. The crossover was defined by a thick layer of photoresist (~ 3 μm). The top plates, dielectric bridges, and transmission lines were gold-plated to a thickness of 3 μm.

After front-side processing, 12 mil via holes for RF grounding were drilled using ultrasonic techniques and then sputtered with gold from the back side, followed by a plated-up process. The last step in the fabrication process was ultrasonic drilling of the rectangular via hole for mounting of the power FET. A specially designed stainless-steel tool was manufactured for drilling the custom-sized rectangular via hole fitting the power FET.

During circuit assembly, the power FET is eutectically (AuSn) mounted on a copper post which protrudes through the rectangular via hole in the substrate. This arrangement allows MMAC processing of the complete circuit on a single substrate at the same time that optimal heat removal from the power FET is accomplished.

Fig. 10 shows the assembled two-stage feedback amplifier. The input Lange coupler is designed in a U shape to reduce circuit dimensions. Although the substrate measures 12.5×5 mm^2, the size has not been optimized, and additional input amplifier stages can possibly be included on the same substrate area.

VI. Measured Results

The feedback amplifier layout allows the circuit to be tested in both open- and closed-loop configurations. The amplifier was first tested in the open-loop configuration, with the feedback circuit terminated with 50 Ω resistors at the junction of the feedback delay line and the coupled

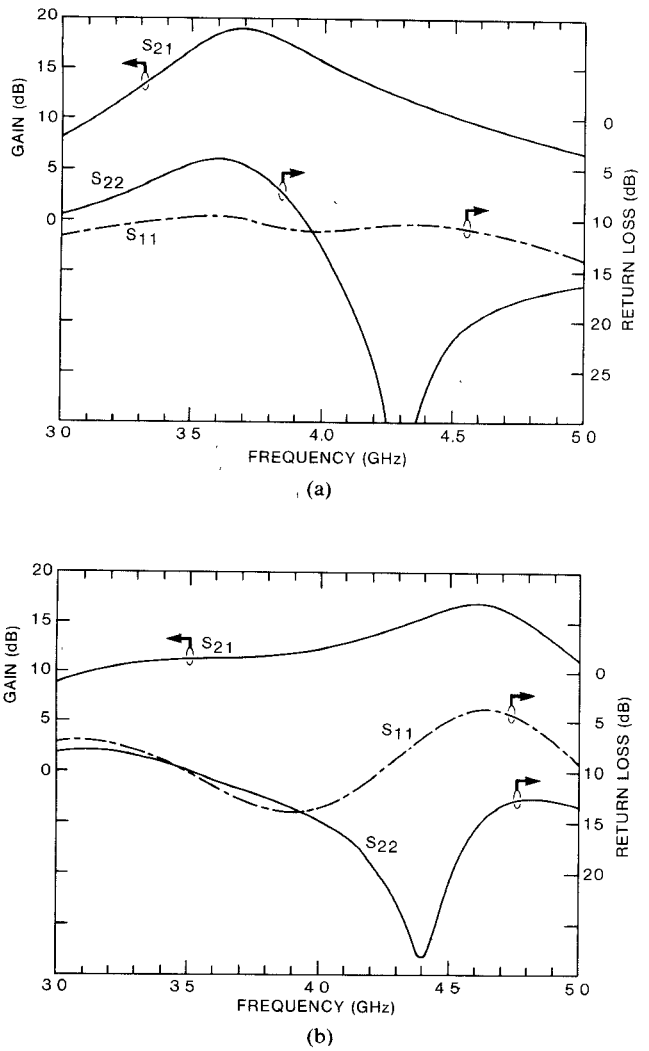

Fig. 11. Measured gain and return loss versus frequency. (a) Without feedback. (b) With feedback.

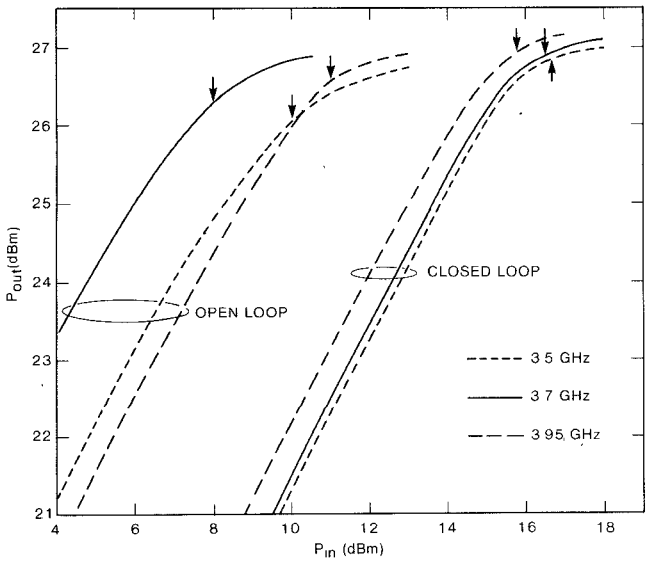

Fig. 12. P_{out} versus P_{in} for both configurations.

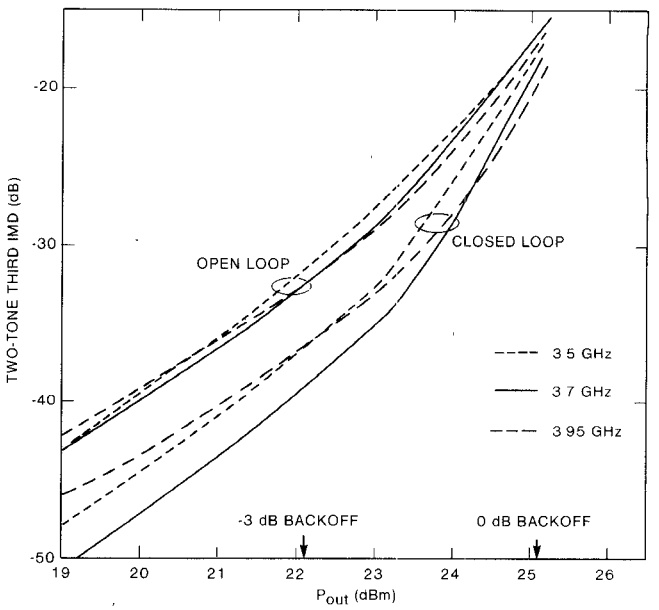

Fig. 13. Third-order IMD versus P_{out}.

TABLE I
KEY OBSERVATIONS FROM MMAC FEEDBACK POWER AMPLIFIER

- Third-order IMD reduced
- Amplifier performance insensitive to large device parameter variation
- Configuration provides good input and output return loss
- Further improvement in performance can be achieved through:
  optimal power design in first stage
  second harmonic trapping in second stage
  operating in optimal class-AB mode

port of the input coupler. The resistors were then disconnected, and the loop was closed to obtain the amplifier data with feedback. The open-loop gain and return losses are shown in Fig. 11(a). The closed-loop gain (Fig. 11(b)) exhibits a decrease in the 3.4–4.2 GHz frequency range. At 3.7 GHz, the drop is as much as 7 dB. The improvement in return loss over that of the open-loop configuration is also shown. These frequency response results show excellent agreement with those obtained from the Supercompact™ calculation, as indicated in Fig. 9.

Fig. 12 shows P_{out} versus P_{in} for both configurations at 3.5, 3.7, and 3.95 GHz. The 1 dB compression point is 0.5 to 1.0 dB higher for the closed loop, and is very close to the saturated power of the amplifier. The data also reveal the effect of feedback in linearizing the amplifier gain. At 4.2 GHz, the difference in value between open- and closed-loop gain is smaller; therefore a smaller improvement was observed for the feedback case. The power-added efficiency at the 1 dB output power compression is ~23%, compared to 20% with no feedback. The input and output return losses are better than 10 dB from 3.4 to 4.2 GHz.

In Fig. 13, the third-order IMD is plotted versus output power for the three frequencies. Again, the improvement in IMD is close to the difference between open- and closed-loop gain for linear power. Near saturation, because of the

drop in amplifier gain, the improvement in IMD is less significant.

The above results show significant improvement of the performance of the two-stage 0.5 W feedback power amplifier at backoff for frequencies between 3.4 and 4.2 GHz. The nominal improvements in the C/I_3 at 3.7 GHz at 0, 3, 6, and 10 dB total input power backoff are 3, 7, 9, and 7 dB, respectively.

Table I presents key observations based on the results for the feedback power amplifier. The third-order IMD improvement, an RF performance that is insensitive to device parameter variation, and good input/output return loss are highlighted based on measured results of the MMAC amplifier. Possible improvement in the power-added efficiency and C/I_3 of the amplifier in the two-stage configuration is suggested. Time-domain simulation has shown that operating the amplifier in class-AB mode will further improve efficiency, as indicated in a more recent study using time-domain analysis [7].

VII. Conclusions

A miniaturized negative-feedback power amplifier for improving linearity at bandwidths exceeding 500 MHz at microwave frequencies has been demonstrated for the first time. A proof-of-concept negative-feedback amplifier experiment was performed that showed improvements in linearity and output power over a narrow bandwidth at 4 GHz. Large-signal analysis of the feedback power amplifier was presented, and the predicted nonlinearity performance of amplifier configurations with and without feedback was obtained. A 3.4–4.2 GHz amplifier was also designed and fabricated using the MMAC technique. The measured results showed good agreement with theoretical predictions.

The MMAC amplifier presented here provides an output power of 27 dBm at 1 dB gain compression, with an improvement of 0.5 to 1.0 dB over the open-loop configuration. The improved linearity is also manifested in a nominal 8 dB improvement in third-order IMD at 3 dB input power backoff. For communications transmitters which are always operated at backoff, an increase in output power at the 1 dB compression point, and improvement in IMD for the negative-feedback design, can be used to enhance overall transmitter efficiency compared to existing systems. Also, the improvement in gain flatness and input/output return losses demonstrates that the feedback technique can be used to simplify the design of power amplifiers which must satisfy stringent specifications. Short-gate-length FET's ($\sim 0.5\ \mu$m) and miniaturized design techniques make it possible to use the negative-feedback technique to obtain good efficiency and higher linearity, as well as improved input and output return losses over the 500 MHz bandwidth used for satellite applications. By combining the negative-feedback technique with class-AB operation of the FET, high linearity and efficient power amplifier performance could be demonstrated in the future.

Appendix

The envelope of the output voltage from an amplifier has a nonlinear relationship with input voltage as

$$V_o(t) = A[V_i(t)]V_i(t) \tag{A1}$$

$$A[V_i(t)] = A_o + \sum_{N=1}^{\infty} A_N V_i^{2N}(t) = \sum_{N=0}^{\infty} A_N V_1^{2N}(t). \tag{A2}$$

A is an even function of V_i since the polarity of the input signal does not affect the gain. For a sinusoidal input, $V_i(t) = V_1 \cos \omega_m t$ and

$$V_o(t) = \sum_{N=0}^{\infty} A_N V_1^{2N+1} \cos^{2N+1} \omega_m t. \tag{A3a}$$

Since

$$\cos^n x = \left(\frac{e^{jx} + e^{-jx}}{2}\right)^n$$

$$= \frac{1}{2^{n+1}} \sum_{l=0}^{n} \binom{n}{l} e^{jnx} e^{-2jls} + \sum_{l=0}^{n} \binom{n}{l} e^{-jnx} e^{2jlx}$$

$$= \frac{1}{2^n} \sum_{l=0}^{n} \binom{n}{l} \cos(n-2l)x \tag{A3b}$$

it follows that

$$V_o(t) = \sum_{N=0}^{\infty} \frac{A_N V_1^{2N+1}}{2^{2N+1}} \sum_{l=0}^{2N+1} \binom{2N+1}{l} \cdot \cos(2N+1-2l)\omega_m t \tag{A3c}$$

$$V_o(t) = \sum_{q=0}^{\infty} \cos[(2q+1)\omega_m t] \sum_{N=q}^{\infty} \frac{A_N V_1^{2N+1}}{2^{2N+1}} \cdot \left[\binom{2N+1}{N-q} + \binom{2N+1}{N+q+1}\right] \tag{A4a}$$

$$V_o(t) = \sum_{q=0}^{\infty} \cos[(2q+1)\omega_m t] \sum_{N=q}^{\infty} \frac{A_N V_1^{2N+1}}{2^{2N}} \binom{2N+1}{N-q} \tag{A4b}$$

$$V_o(t) = \sum_{q=0}^{\infty} B_{2q+1}(V_1) \cos[(2q+1)\omega_m t] \tag{A4c}$$

$$\frac{C}{I_3} = \frac{B_1(V_1)}{B_3(V_1)}. \tag{A5}$$

Acknowledgment

The authors would like to thank J. Singer and G. Tough for the RF measurements and K. Hogan for circuit fabrication. They also wish to thank D. Sachdev and K. Betaharon for valuable technical discussions and suggestions.

References

[1] A. Ezzeddine, H-L. A. Hung, and H. C. Huang, "High-voltage FET amplifiers for satellite and phased-array applications," in *IEEE MTT-S Int. Microwave Symp. Dig.* (St. Louis, MO), June 1985, pp. 336–339.

[2] A. A. M. Saleh and M. F. Wazowicz, "Efficient, linear amplification of varying-envelope signals using FET's with parabolic transfer characteristics," *IEEE Trans. Microwave Theory Tech.*, vol. MTT-33, pp. 703–710, Aug. 1985.
[3] K. B. Niclas, W. T. Wilser, R. B. Gold, and W. R. Hitchens, "The matched feedback amplifier ultrawide-band microwave amplification with GaAs MESFETs," *IEEE Trans. Microwave Theory Tech.*, vol. MTT-28, pp. 285–294, Apr. 1980.
[4] K. Honjo, T. Sugiura, and H. Itoh, "Ultra-broad-band GaAs monolithic amplifier," *IEEE Trans. Microwave Theory Tech.*, vol. MTT-30, pp. 1027–1033, July 1982.
[5] C. C. Hsieh and E. Strid, "An *S*-band high power feedback amplifier," in *IEEE MTT-S Int. Microwave Symp. Dig.* (San Diego, CA), June 1977, pp. 182–184.
[6] M. Takahashi, N. Asari, and S. Aihara, "A negative feedback amplifier in microwave frequencies," *NEC Res. Develop.*, no. 77, pp. 63–69, Apr. 1985.
[7] J. Gross, H-L. Hung, and G. Hegazi, "Time-domain analysis of C-band Class-AB feedback power FET amplifier," COMSAT Laboratories Tech. Note MED/86-023, COMSAT Data Catalog No. 86DC085, Sept. 1986.

✠

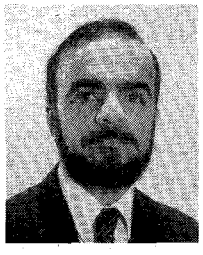

Amin K. Ezzeddine (S'78–M'82) was born in Cairo, Egypt, in 1953. He attended the School of Engineering at Ain Shams University in Cairo and obtained the bachelor of science degree in electrical engineering in 1976. He received both the master of science and doctor of science degrees from the Massachusetts Institute of Technology, Cambridge, in 1979 and 1983, respectively.

He taught at Ain Shams University from 1976 to 1977. In 1982, he joined COMSAT Laboratories as a Member of the Technical Staff and he worked in microwave circuit development. In 1986, he joined the Tachonics Corporation as a Principal Engineer and contributed to the design and development of a variety of GaAs MMIC products. In 1988, he rejoined COMSAT Laboratories as Scientist working on MMIC development and is currently Associate Manager in the Microwave Components Division. His current interests are in MIMIC circuit design, numerical modeling of microwave passive and active circuits, and electrodynamics phenomena.

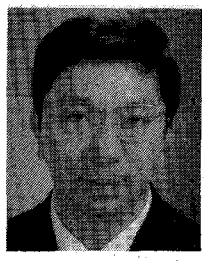

Hing-Loi A. Hung (S'67–M'75–SM'81) received the S.B.E.E. degree from the Massachusetts Institute of Technology in 1968 and the M.S. and Ph.D. degrees from Cornell University, Ithaca, NY, in 1970 and 1974, respectively.

He joined COMSAT Laboratories in 1974 and is currently Manager of the Monolithic Microwave Techniques Department of the Microwave Components Division, Clarksburg, MD. His present research areas include millimeter-wave monolithic integrated circuits, heterojunction devices, optoelectronics/microwave techniques, and MMIC reliability. He participated in satellite transponder designs for the INTELSAT V and VI and COMSAT STC programs.

Dr. Hung has been a Professorial Lecturer at George Washington University since 1978, and was Vice-Chairman and Chairman of the IEEE Electron Devices Society, Washington Section, from 1980 to 1982.

✠

Ho C. Huang (M'68–SM'80) received the B.S.E.E. degree from National Taiwan University in 1959 and the M.S. and Ph.D. degrees from Cornell University, Ithaca, NY, in 1965 and 1967, respectively.

He is currently Director of the Microelectronics Division at COMSAT Laboratories, Clarksburg, MD, where his responsibilities include research in III–V compound semiconductor materials, microwave device and circuit design, MIC and MMIC fabrication technology, and physical/chemical analysis. Prior to joining COMSAT in 1983, he was with RCA Laboratories.

Dr. Huang has served as Session Chairman for many IEEE technical conferences, and has been awarded seven U.S. patents. In 1983, he was granted the David Sarnoff Award for Outstanding Technical Achievement.